In Vitro Cellular & Developmental Biology - Animal
https://doi.org/10.1007/s11626-024-00960-w

Ginsenoside Rg1 treats chronic heart failure by downregulating ERK1/2 protein phosphorylation

Liqi Peng[1] · Shaodong Li[2] · Huzhi Cai[3] · Xueliang Chen[2] · Yanping Tang[2]

Received: 16 December 2023 / Accepted: 22 July 2024 / Editor: Tetsuji Okamoto

Abstract
In this study, we investigated the potential therapeutic mechanism of ginsenoside Rg1 (GRg1) in chronic heart failure (CHF), focusing on its regulation of ERK1/2 protein phosphorylation. H9c2 cardiomyocytes and SD rats were divided into the control group, CHF (ADR) group, and CHF+ginsenoside Rg1 group using an isolated cardiomyocyte model and an in vivo CHF rat model induced by adriamycin (ADR). Cell viability, proliferation, apoptosis, and the expression of relevant proteins were measured to assess the effects of GRg1. The results showed that treatment with GRg1 increased cell activity and proliferation, while significantly reducing levels of inflammatory and apoptotic factors compared to the CHF (ADR) group. Moreover, the CHF+ginsenoside Rg1 group exhibited higher levels of Bcl-2 mRNA and protein expression, as well as lower levels of Caspase3 and Bax mRNA and protein expression, compared to the CHF (ADR) group. Notably, the CHF+ginsenoside Rg1 group displayed decreased serum NT-proBNP levels and heart weight/body weight (HW/BW) index. Furthermore, the electrocardiogram of rats in the CHF+ginsenoside Rg1 group resembled that of rats in the control group. Overall, our findings suggested that GRg1 alleviated CHF by inhibiting ERK1/2 protein phosphorylation, thereby inhibiting apoptosis, enhancing cell activity and proliferation, and reducing cardiac inflammatory responses.

Keywords Ginsenoside Rg1 · ERK1/2 · Chronic heart failure · Apoptosis · Adriamycin

Introduction

Chronic heart failure (CHF) poses a considerable global health challenge, impacting a substantial population. Epidemiological studies indicate that CHF has a prevalence of approximately 3–5% in adults (McDonagh *et al*. 2021), and the prognosis for patients is often grim, with a mere 50% 5-yr survival rate (Stretti *et al*. 2021). Although traditional medications used to treat CHF have shown some effectiveness in improving patient outcomes, they are still bound by limitations that contribute to elevated rates of mortality and hospital readmissions. Consequently, an urgent imperative exists to uncover novel drugs, identify potential therapeutic targets, and explore innovative treatment strategies in order to effectively combat this pressing health concern of CHF.

The extracellular regulated protein kinase1/2 (ERK1/2) signaling pathway occupies a crucial role in regulating cardiac hypertrophy induced by various factors, including angiotensin II (Ang II), endothelin-1 (ET-1), and stress load (He *et al*. 2018; Huang *et al*. 2018; Zhouming *et al*. 2021). Previous investigations have demonstrated a notable upregulation of phosphorylated ERK1/2 (p-ERK1/2) expression in the myocardial tissue of rats with CHF caused by adriamycin (ADR) (Yang *et al*. 2020; Yan *et al*. 2021). Furthermore, a study conducted by Ye *et al*. showed that the deletion of the CMTM3 gene deletion modulated the MAPK/ERK pathway, thereby exacerbating cardiac insufficiency induced by Ang II (Ye *et al*. 2023). Wang *et al*. demonstrated that LCZ696 effectively reduced the expression of apoptotic signaling molecules by suppressing ERK phosphorylation, consequently attenuating cardiac injury (Wang *et al*. 2019). Additionally, Ju *et al*. showed that overexpression of LRP1

Liqi Peng and Shaodong Li are co-first authors.

✉ Yanping Tang
tangyp@hnucm.edu.cn

1 First Clinical College of Traditional Chinese Medicine, Hunan University of Chinese Medicine, Changsha 410007, Hunan, China

2 Hunan University of Chinese Medicine, Changsha 410208, Hunan, China

3 The First Hospital of Hunan University of Chinese Medicine, Changsha 410007, Hunan, China

Published online: 09 September 2024

upregulated protein kinase Cα, which in turn activates ERK and ultimately leads to cardiac hypertrophy (Ju *et al*. 2020). In summary, inhibiting the activation of the ERK1/2 signaling cascade holds promise as a potential approach to alleviating myocardial hypertrophy in CHF.

Ginsenoside Rg1 (GRg1), a prominent bioactive constituent derived from *ginseng*, has been demonstrated to exhibit a diverse array of beneficial effects including anti-aging, anti-inflammatory, anti-apoptotic, and antioxidant properties (Cai *et al*. 2022; Sun *et al*. 2022). An accumulating amount of evidence substantiates the notion that GRg1 plays a pivotal role in safeguarding the cardiovascular system. Studies have demonstrated its ability to inhibit Ang II-induced myocardial hypertrophy, attenuate cardiomyocyte apoptosis and inflammatory responses, and ameliorate ADR-induced cardiac dysfunction (Xu *et al*. 2018; Luo et al. 2020; Guan *et al*. 2023). Mechanistically, GRg1 has been demonstrated to regulate both the MAPK and ERK signaling pathways (Huang *et al*. 2016; Zhu *et al*. 2017; Xie *et al*. 2018; Liu *et al*. 2022a). Yuan *et al*. revealed that GRg1 could mitigate diabetes-induced myocardial ischemia-reperfusion injury (I/R) by modulating the ERK signaling pathway and activating HIF-1α (Yuan *et al*. 2019). Furthermore, research conducted by He *et al*. demonstrated that GRg1 can suppress shear-induced inflammatory reactions by impeding the MAPK signaling pathway (He and Li 2015). Consequently, it is our proposal that GRg1 may exert a protective effect against myocardial injury in chronic heart failure through modulation of the ERK1/2 signaling pathway. Nevertheless, the precise molecular mechanisms through which GRg1 controls the phosphorylation of ERK1/2 proteins remain unclear.

In the present study, we sought to delve deeper into the potential of GRg1 in mitigating and managing chronic heart failure. To accomplish this, we performed a series of cellular and animal experiments to investigate the impact of GRg1 on ERK1/2 phosphorylation levels in cardiomyocytes and myocardial tissues. These investigations have provided us with a novel theoretical framework as well as a promising therapeutic target for the prevention and treatment of CHF.

Materials and methods

In vitro experiment - Cell culture and treatment The H9c2 cardiomyocyte cell line was sourced from the Cell Bank of the Chinese Academy of Sciences (Shanghai, China). Prior to experimentation, cells were cultured in serum-free DMEM for a duration of 24 h. To establish an in vitro model simulating CHF, the H9c2 cardiomyocytes were subjected to two rounds of washing with D-Hanks solution. Subsequently, the cells were exposed to serum-free media supplemented with 0.1 mol/L doxorubicin (DOX), also known as ADR, for a duration of 6 h. As previously described (Li *et al*. 2017; Lu *et al*. 2015); H9c2 cardiomyocytes in the CHF+ginsenoside Rg1 group were then pretreated with GRg1 (40 μM). Afterwards, the H9c2 cardiomyocytes were categorized into three distinct groups in a randomized manner: the normal control group, the CHF (ADR) group, and the CHF+ ginsenoside Rg1 group.

3-(4,5-Dimethylthiazol-2-yl)-2,5-diphenyltetrazolium bromide assay (MTT) The viability of H9c2 cardiomyocytes in each group was assessed using an MTT kit (HG-M100, HonorGene, Changsha, China). Tryptic digest was used to break down the cardiomyocytes and create cell suspensions. With three duplicate wells for each group, the cardiomyocytes were seeded onto 96-well plates at a dosage of 1×10^4/100 μL. The cardiomyocytes were intervened and treated according to the aforementioned experimental grouping, followed by a 24-h culture period, and 5 mg/mL MTT was applied to each well after that. The cardiomyocytes were centrifuged to remove the supernatant after being cultured for 4 h at 37°C and 5% CO_2. Following this, 150 μL of dimethyl sulfoxide was added to each well and thoroughly mixed. On a Bio-Tek Enzyme Marker (MB-530, Shenzhen Huisong Technology Development Co., Ltd., Shenzhen, China), the absorbance at 490 nm (OD) was measured.

5-Ethynyl-2′-deoxyuridine (EdU) assay Cardiomyocyte proliferation in each experimental group was assessed using the EdU kit (C00054, Guangzhou RiboBio Co., Ltd., Guangzhou, China) in accordance with the manufacturer's instructions. To initiate the experiment, EdU was diluted to a concentration of 50 μM and subsequently added to the cell culture medium. After a 24-h incubation period, the medium was discarded, and the cells were carefully washed. A 4% paraformaldehyde solution (100 μL) was added to each well and incubated for 30 min at room temperature. Then, 100 μL of Triton X-100 was added to each well, and the cells were incubated on a decolorizing shaker for 10 min, followed by another round of washing. Subsequently, 100 μL of 1× Apollo® Staining Reaction Solution was added, and the cardiomyocytes were incubated in a decolorizing shaker, shielded from light, at room temperature for 30 min. For DNA staining, a 100 μL portion of 1× Hoechst 33342 reaction solution was employed under dark conditions. Finally, cells in each experimental group were observed using a fluorescence microscope (BA410T, Motic, Xiamen, China). Five random fields of view were selected and documented for per well.

Flow cytometry Apoptosis assessment was conducted in the various groups of cardiomyocyte using the Annexin V-FITC Apoptosis Detection Kit (KGA108, Jiangsu Keygen Biotech Corp., Ltd., Nanjing, China), following the established protocols. Initially, trypsin digestion was employed to detach

the cardiomyocytes, followed by centrifugation at 4°C and 1500 rpm for 5 min using a low-speed centrifuge (SL02, Shanghai Zhixin Experimental Instrument Technology Co., Ltd., Jiaxing, China). The supernatant was cautiously eliminated through washing. To suspend the cardiomyocytes, 500 μL of Binding Buffer was added, followed by the addition and incubation of 5 μL of Annexin V-FITC and 5 μL of propidium iodide. The mixture was then allowed to react at room temperature, protected from light, for a duration of 5–15 min. Flow cytometry (A00-1-1102, Beckman, Brea, CA) was employed. Each set of experiments was performed in triplicate experiments to ensure reliable results.

Real-time quantitative PCR (RT-qPCR) Total cellular RNA was extracted utilizing the Trizol reagent (15596026, Thermo, Waltham, MA) in accordance with the manufacturer's instructions. The cDNA synthesis was carried out using the reverse transcription kit (CW2569, Beijing ComWin Biotech Co., Ltd., Beijing, China). The RT-qPCR reaction system was prepared implementing the cDNA as a template. The levels of Caspase3, Bax, and Bcl-2 mRNA expression in cardiomyocytes were measured using a real-time fluorescence quantitative PCR instrument (QuantStudio1, Thermo). The parameters for the quantitative PCR amplification reaction were as follows: pre-denaturation occurred at a temperature of 95°C for a duration of 10 min, denaturation was performed at 95°C for a period of 15 s, and annealing took place at 60°C for 0.5 min. A total of 40 cycles were performed. The expression levels of Caspase3, Bax, and Bcl-2 mRNA in the cardiomyocytes were quantified using the $2^{-\Delta\Delta Ct}$ method with actin as an internal reference. The amplification primers used are shown in Table 1..

Immunofluorescence (IF) To visualize the expression of ERK1/2 and p-ERK1/2 in cardiomyocytes, an IF technique was employed. Cell crawling tablets were thoroughly cleaned using phosphate-buffered saline (PBS) for two to three times, followed by fixation using 4% paraformaldehyde for 30 min. After that, the samples were treated with 0.3% Trilatone at 37°C for 30 min to allow permeabilization.

Table 1. Primers' sequences

Gene	Sequence
β-Actin	F: ACATCCGTAAAGACCTCTATGCC
	R: TACTCCTGCTTGCTGATCCAC
Caspase3	F: ATCAGCCTAATTTTACAGACC
	R: TCTCCTTTCCTTACGCTCT
Bax	F: TTGCTACAGGGTTTCATCCAGG
	R: GCTCCAAGGTCAGCTCAGGT
Bcl-2	F: CTGGTGGACAACATCGCTCT
	R: ATAGTTCCACAAAGGCATCCCA

Blocking of the tablets was achieved by incubating them with 5% BSA at 37°C for 60 min. The primary antibodies, including anti-rabbit ERK1/2 (ab184699, Abcam, Cambridge, UK) and anti-rabbit p-ERK1/2 (bs-14624r, Bioss, Beijing, China), were diluted at a 1:50 dilution and were added to the tablets and allowed to incubate overnight at 4°C. Following this, fluorescently labeled secondary antibody, anti-rabbit IgG (SA00013-2, Proteintech, Rosemont, IL) at a 1:200 dilution, was drop-wise added to the samples and incubated for 90 min at 37°C. To visualize the nuclei, a DAPI working solution was applied and incubated for 10 min at 37°C in the dark. After three washes with PBS for 5 min each, the sections were sealed with buffered glycerol. Finally, the staining images were observed and captured using a fluorescence microscope computer (BA410T, Motic, Xiamen, China). ERK1/2 and p-ERK1/2 are green fluorescence and nuclear staining signals showed blue fluorescence. The number of total cells and positive cells was measured respectively, and the integrated optical density (IOD) value was measured.

Western blotting The levels of Caspase3, Bax, Bcl-2, ERK1/2, and p-ERK1/2 proteins in the cells were assessed through Western blotting analysis. Total cellular proteins were extracted using RIPA lysis buffer from Beyotime (P0013B, Shanghai, China). The BCA protein quantification kit from Abcam (ab287853) was utilized to measure the protein concentration, as per the guidelines provided by the manufacturer. A 100-μL aliquot of the protein supernatant was collected and subjected to denaturation by being boiled in water for 5 min. Electrophoresis was performed using the DYY-6C system from Beijing Liuyi Biotechnology Co., Ltd. (Beijing, China), maintaining a constant voltage of 75 V for a period of 130 min. Subsequently, the protein samples from each group were transferred to a PVDF membrane using the DYCZ-40D membrane transfer apparatus, also from Beijing Liuyi Biotechnology Co., Ltd. The PVDF membrane was incubated with appropriately diluted primary antibodies overnight at a temperature of 4°C. The secondary antibodies, labeled with HRP, were diluted in 1× PBST and incubated with the PVDF membrane at room temperature for 90 min. Chemiluminescent detection was carried out using the ECL system from Shanghai Qinxiang Scientific Instrument Co., Ltd. (Chemiscope6100, Shanghai, China). The PVDF membrane was co-incubated with the ECL chemiluminescent solution for 1 min, followed by exposure to X-ray film in a dark box. The film was subsequently developed and rinsed. Table 2. shows the information of primary and secondary antibodies.

In vivo experiments - Experimental animals and handling Fifty SPF-grade healthy male SD rats, aged 6 wk, with an average weight of 180 ± 10 g, were selected for

Table 2. Antibodies' information

Name	Dilution	Manufacturer	Catalog Number
Caspase3	1:1000	CST, USA	#9664
Bax	1:500	Proteintech, USA	50599-2-lg
Bcl-2	1:200	Proteintech, USA	12789-1-AP
ERK1/2	1:10,000	Abcam, UK	ab184699
p-ERK1/2	1:1000	Bioss, China	bs-14624r
HRP-labeled Goat anti-mouse IgG (secondary antibody)	1:5000	Proteintech, USA	SA00001-1
HRP-labeled Goat anti-rabbit IgG (secondary antibody)	1:6000	Proteintech, USA	SA00001-2
TNFα	1:1000	Abcam, UK	ab6671
IL-6	1:1000	Bioss, China	bs-0782R
HMGB1	1:1000	Abcam, UK	ab18256

this study. These rats were obtained from the Laboratory Animal Center of Hunan University of Chinese Medicine. To induce HF in the rats, ADR hydrochloride was used for injection, which was diluted to a concentration of 1.0 mg/mL using 0.9% NaCl solution for intraperitoneal injection. Each rat was given a weekly dose of 2 mg/kg for a duration of 6 wk, resulting in a cumulative total dose of 12 mg/kg. Before each administration, the body weight of rats was re-measured to ensure accurate dosage calculation. To assess the success of the in vivo modeling of congestive CHF in the rats, measurements of cardiac function were performed at the end of week 6, serving as an indicator of the effectiveness of the CHF model.

Grouping and drug administration After a week of acclimatization, a total of 30 SD rats were included. Ten of them were randomly assigned to form the normal control group, while the remaining 20 rats were used to replicate the CHF rat model using the previously described modeling method. Cardiac function measurements were performed at the end of the modeling period and continued throughout the sixth week. Based on the results, the rats were randomly divided into two groups: the CHF (ADR) group and the CHF+ginsenoside Rg1 group. Starting from the seventh week, rats were administered intraperitoneal injections according to their group assignment. The doses were calculated using the human-mouse body surface area method to ensure accurate conversion. The rats in the CHF+ginsenoside Rg1 group received a daily dose of GRg1 at 20 mg/kg, while the rats in the normal control and CHF (ADR) groups were injected with the same volume of 0.9% saline. This injection regimen was performed once daily for a duration of 4 wk, as previously described (Yu *et al*. 2016).

Electrocardiogram (ECG) Four weeks after the dosing, electrocardiograms (ECGs) were conducted. All the examinations were performed by the same sonographer, who remained unaware of the animal grouping during the examination process. In the case of CHF rats, anesthesia was induced using sodium pentobarbital at a dose of 30 mg/kg, following the previously described protocol (Zhang *et al*. 2022). The rats were positioned supine on the experimental table and securely restrained. Subcutaneous electrodes were appropriately placed in the standard rat limb lead II position to accurately record the ECG. The LabChart software (version 7.3, AD Instruments Pty Ltd, Bella Vista, Australia) was utilized to assess the ECG recordings, focusing on parameters such as P-wave duration, PR interval, QRS duration, and corrected QT interval (QTc).

Enzyme-linked immunosorbent assay (ELISA) Serum NT-proBNP levels of the rats in each group were quantified using an ELISA following standard protocols. After the rats were anesthetized, they were euthanized via spinal subluxation. Blood was collected from the abdominal aorta and transferred into a centrifuge tube. The tube was left at room temperature for 1 h to allow for proper coagulation. Following centrifugation at 3200 r/min for 35 min, the supernatant was carefully collected. To determine the levels of NT-proBNP, the optical density (OD) value of each sample was determined using the ELISA kit (CSB-E08752r, CUSABIO, Wuhan, China) at a wavelength of 450 nm as per the provided instructions. A standard curve was constructed using the concentration of the standard as the vertical axis and the corresponding OD values as the horizontal axis. The professional curve software "Curve Expert" was utilized for the analysis of the standard curve. By establishing the regression equation based on the concentration of the standard versus the OD value, the NT-proBNP concentration in each sample was able to be calculated by substituting the sample's OD value into the equation.

Heart weight/body weight Index (HW/BW) Prior to euthanasia, the body weight (BW) of the rats was recorded. Subsequently, their heart tissues were carefully obtained, cleansed, and weighed (HW) using a chilled saline solution. To calculate the heart weight/body weight index, the ratio of HW to BW was multiplied by 100%.

Terminal deoxynucleotidyl transferase dUTP nick end labeling (TUNEL) Cardiomyocyte apoptosis in each experimental group was assessed employing the Tunel kit (40306ES50, Shanghai Yeasen biotech Co., Ltd., Shanghai, China), as per the manufacturer's instructions. The tissue sections were meticulously dewaxed and hydrated, and treated with 100 μL of Proteinase K working solution for a 20-min reaction at 37°C. To ensure thorough rinsing, the sections were

immersed in 1× PBS solution for three consecutive cycles. For the TUNEL assay, a solution containing TdT enzyme and FITC-12-DUTP labeling mixture was meticulously prepared. This TUNEL assay solution was then cautiously added to each sample, followed by incubation in the dark at 37°C for 60 min. After thorough washing with PBS for three times, the samples were stained with DAPI (5 μg/mL) to visualize the nuclei, with a continued incubation period of 10 min. The DAPI staining solution was subsequently aspirated, and another round of three PBS washes was performed. The occurrence of cardiomyocyte apoptosis in each experimental group was observed under a fluorescence microscope (BA410T, Motic).

RT-qPCR The mRNA levels of Caspase3, Bax, and Bcl-2 in the myocardial tissues were measured using a RT-qPCR instrument (QuantStudio1, Thermo) following the same detection method as described in "Real-time quantitative PCR (RT-qPCR)" section.

IF IF analysis was employed to observe the expression levels of ERK1/2 and p-ERK1/2 in the myocardial tissue of rats with CHF in each experimental group. Tissue sections were prepared by undergoing a series of steps. Firstly, they were immersed in xylene for 20 min, repeated three times, to remove the wax. Subsequently, the sections were hydrated. The sections underwent thermal antigen retrieval by immersing them in EDTA (pH 9.0) solution, followed by cooling, and washing with 0.01 M PBS (pH 7.2–7.6) for 3 min, repeated three times. The slices were then treated with sodium borohydride solution at room temperature for a duration of 30 min, followed by rinsing in water for 5 min. To block the sections, a mixture of 10% normal serum and 5% BSA was applied and left for 60 min. The subsequent steps of the assay were carried out following the protocol described in the "Immunofluorescence (IF)" section.

Western blotting The protein expression levels of Caspase3, Bax, Bcl-2, ERK1/2, and p-ERK1/2 as well as the inflammatory factors TNFα, HMGB1, and IL-6 in the myocardial tissues of rats with CHF in each experimental group were assessed using Western blotting. In addition to the primary antibodies specified, the following antibodies were utilized: anti-rabbit TNFα (1:1000, ab6671, Proteintech), anti-rabbit IL-6 (1:1000, bs-0782R, Bioss), and anti-rabbit HMGB1 (1:1000, ab18256, Abcam). The remaining steps of the procedure, including the selection of secondary antibodies, were carried out as previously described in the "Western blotting" section.

Statistical analysis All collected data in this study were subjected to normality testing and were subsequently statistically analyzed using SPSS 27.0 (IBM, Armonk, NY). Measurements that demonstrated a normal distribution were reported as mean ± standard deviation (s). Comparisons among multiple means were assessed using one-way analysis of variance (ANOVA) in accordance with the nature of the study. Prior to the ANOVA, Levene's test for chi-squared was conducted to ensure homogeneity of variances. A p-value of less than 0.05 was considered to indicate statistical significance.

Results

Ginsenoside Rg1 affects cardiomyocyte proliferation To investigate the impact of ginsenoside Rg1 (GRg1) on cardiomyocyte proliferation, an in vitro model of CHF was established using ADR. Cell viability and proliferation in each group were assessed using MTT assay and EdU staining, respectively. The results obtained from the MTT assay demonstrated a noticeable decrease in cell viability in both the CHF (ADR) group and the CHF+ginsenoside Rg1 group, when compared to the control group of normalcy ($p < 0.01$). Notably, the reduction in cell viability was more pronounced in the CHF (ADR) group ($p < 0.01$, Fig. 1*A*). Furthermore, the EdU assay demonstrated a reduced count of proliferating cells in both the CHF (ADR) group and the CHF+ginsenoside Rg1 group, compared to the control group ($p < 0.01$). Importantly, the cell proliferation rate in the CHF+ginsenoside Rg1 group was significantly higher than that in the CHF (ADR) group ($p < 0.01$, Fig. 1*B*). These findings suggested that ADR-induced CHF leads to a dramatic decrease in cell viability, while the administration of GRg1 was beneficial in enhancing cell proliferation rate and alleviating myocardial injury in CHF.

Ginsenoside Rg1 affects cardiomyocyte apoptosis To explore the safeguarding impact of GRg1 against cellular apoptosis, we conducted flow cytometry analysis to detect apoptosis. Additionally, we utilized RT-qPCR and Western blotting methodologies to evaluate the expression levels of Caspase3, Bax, and Bcl-2 mRNA and protein in cells from each experimental group. The flow cytometry data revealed that administration of ADR promoted cell apoptosis in the induced CHF model. The apoptosis rate was significantly elevated in both the CHF (ADR) and CHF+ginsenoside Rg1 groups as compared to the normal control group ($p < 0.01$). Importantly, treatment with GRg1 demonstrated a notable reduction in ADR-induced apoptosis ($p < 0.01$, Fig. 2*A*). RT-qPCR analysis revealed a notable decrease in Bcl-2 mRNA expression in the CHF (ADR) cohort in comparison to the other two cohorts ($p < 0.01$), while the expression levels of Caspase3 and Bax mRNA in the CHF (ADR) group were higher relative to the other two groups ($p < 0.01$, Fig. 2*B*). Western blotting revealed that ADR induction resulted in

enhancement of Caspase3 and Bax protein expression, along with reduction of Bcl-2 protein expression in cardiomyocytes across all groups ($p < 0.01$, Fig. 2*C*). Interestingly, the expression level of Bcl-2 protein was significantly upregulated in the CHF+ginsenoside Rg1 group compared to the CHF (ADR) group ($p < 0.01$, Fig. 2*C*), indicating that GRg1 can effectively inhibit cell apoptosis in CHF.

Ginsenoside Rg1 regulates ERK1/2 protein phosphorylation To explore the potential involvement of GRg1 in the inhibition of ERK1/2 protein phosphorylation in the treatment of CHF, the expression levels of ERK1/2 and p-ERK1/2 proteins in cardiomyocytes were examined using Western blotting. The distribution of ERK1/2 and p-ERK1/2 was detected through IF staining. The level of p-ERK1/2 proteins was substantially higher in the CHF (ADR) group in contrast to the normal control group, while it was reduction in the CHF+ginsenoside Rg1 group ($p < 0.01$, Fig. 3*A*). The CHF (ADR) group exhibited the highest ratio of p-ERK1/2 to ERK1/2 ($p < 0.01$). However, ginsenoside Rg1 reversed the increase. IF staining using antibodies against ERK1/2 and p-ERK1/2 (green) in combination with DAPI staining for cardiomyocyte nuclei (blue) further supported these findings (Fig. 3*B*). The mean fluorescence intensity of ERK1/2 was obtained by measuring the luminosity of the positive areas divided by the positive area. The results showed that there was no significant difference among the three groups. The positive rate of p-ERK1/2 was calculated by measuring the number of positive cells out of the total number of cells. Statistical analysis revealed a significant difference in the positive rate of p-ERK1/2 among the normal control group, CHF (ADR) group, and CHF+ginsenoside Rg1 group ($p < 0.01$). The positive rate of p-ERK1/2 was significantly increased in the CHF (ADR) group. However, the positive rate of p-ERK1/2 in the CHF+ginsenoside Rg1 group was suppressed compared with the CHF group. These results suggested that GRg1 may exert its cardioprotective effects by inhibiting ERK1/2 protein phosphorylation, which can enhance cardiomyocyte proliferation and reduce cell apoptosis.

Protective effects of ginsenoside Rg1 in the heart of rats with CHF In this study, the myocardial injury model of CHF rats was replicated by the ADR induction method. The protective effect of GRg1 on the heart of CHF rats was confirmed by electrocardiography, ELISA assay, and Western blotting. As shown in Fig. 4*A*, abnormalities were observed in the limb II electrocardiogram (ECG) of rats in the CHF (ADR) group, with the QRS wave direction being opposite to that of the normal control group and CHF+ginsenoside Rg1 group. The levels of NT-proBNP in rat serum serve as indicative of the extent of myocardial injury. ELISA results demonstrated a marked elevation in serum NT-proBNP levels in both the CHF (ADR) group and the CHF+ginsenoside Rg1 group compared to the control group ($p < 0.01$, Fig. 4*B*). Notably, the elevation in the CHF (ADR) group was more pronounced ($p < 0.01$). Western blotting analysis revealed a remarkable decrease in the expression of TNFα, HMGB1, and IL-6 in myocardial tissue from rats in the CHF+ginsenoside Rg1 group compared to the CHF (ADR) group ($p < 0.01$, Fig. 4*C*). These findings confirmed the ability of GRg1 to regulate key inflammatory factors involved in myocardial function.

Effect of ginsenoside Rg 1 on cardiac apoptosis in CHF rats In this investigation, the defensive impact of GRg1 on cardiac apoptosis in rats with CHF was examined. To assess this effect, we measured the HW/BW index, apoptosis rate, and the expression levels of Caspase3, Bax, and Bcl-2 mRNA and proteins in experimental rats. The HW/BW index of CHF rats is shown in Fig. 5*A*. The HW/BW index of the CHF (ADR) group exhibited a significantly higher value

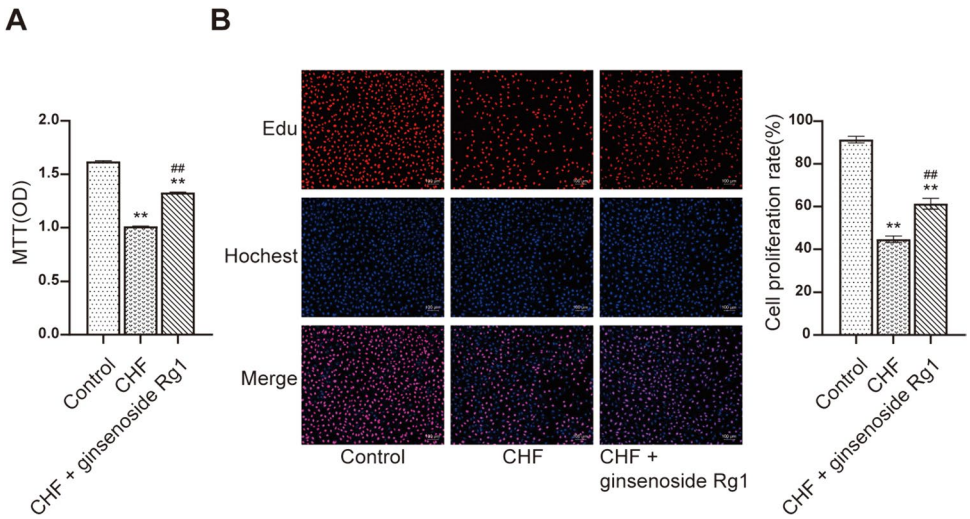

Figure 1. Impact of GRg1 on cardiomyocyte proliferation. (*A*) Evaluation of cardiomyocyte survival rate using the MTT method. (*B*) EdU analysis of cardiomyocyte proliferation rate assessment (*scale bar*: 100 μm). (**$p < 0.01$ denotes a substantial distinction when compared to the control group, $^{\#\#}p < 0.01$ denotes a substantial difference compared to the CHF (ADR) group).

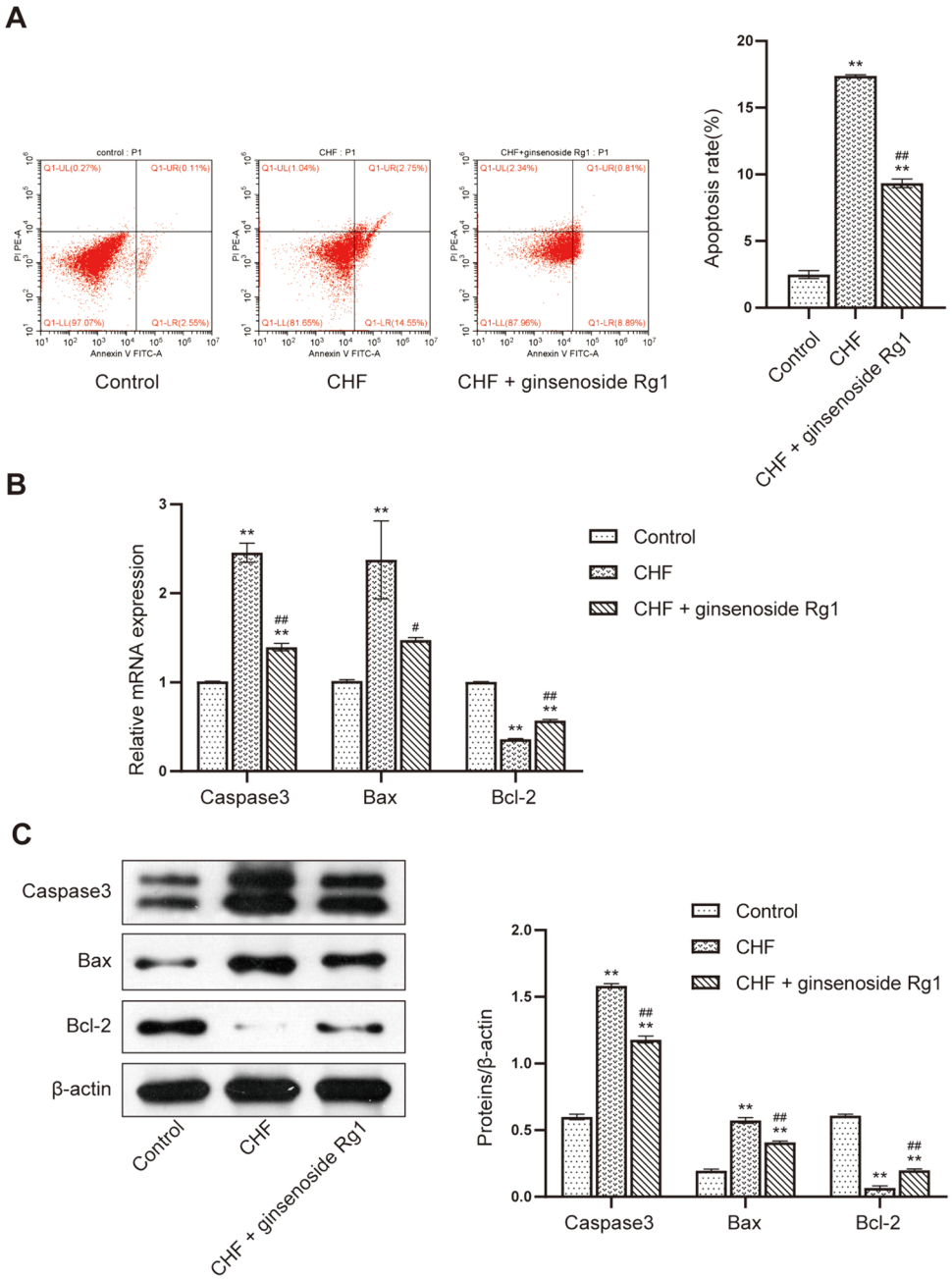

Figure 2. Influence of GRg1 on cardiomyocyte apoptosis. (*A*) Apoptosis assessment conducted by flow cytometry. (*B*) Quantification of Caspase3, Bax, and Bcl-2 mRNA expression in cardiomyocytes using RT-qPCR. (*C*) Analysis of Caspase3, Bax, and Bcl-2 protein expression in cardiomyocytes by Western blotting. (**$p < 0.01$ indicates a significant difference compared to the control group, $^{\#}p < 0.05$ and $^{\#\#}p < 0.01$ indicate a significant difference compared to the CHF (ADR) group).

than that of the normal control group ($p < 0.01$). The HW/BW index of the CHF+ginsenoside Rg1 group was intermediate between the control and the CHF (ADR) group. Furthermore, we evaluated the apoptosis rate in these groups, which is presented in Fig. 5*B*. The CHF (ADR) group exhibited the highest apoptosis rate, followed by the CHF+ginsenoside Rg1 group. There was a statistical significance in the difference of apoptosis rates among the three groups ($p < 0.01$). To further investigate the underlying mechanisms, we analyzed the mRNA and protein expression levels of Bcl-2, Caspase3, and Bax. RT-qPCR and Western blotting consistently revealed that the CHF (ADR) group had significantly lower levels of Bcl-2 mRNA and protein expression compared to the normal control group and the CHF+ginsenoside Rg1 group. Conversely, the Caspase3 and Bax mRNA and protein expression levels were significantly higher in the CHF (ADR) group than in the other two groups ($p < 0.01$, Fig. 5*C*, *D*). These findings confirmed that GRg1 could effectively improve ventricular remodeling and inhibit cardiomyocyte apoptosis in rats with CHF.

Ginsenoside Rg1 regulates ERK1/2 protein phosphorylation in CHF rats To elucidate the protective effects of GRg1 on the ADR-induced CHF rat model and its underlying

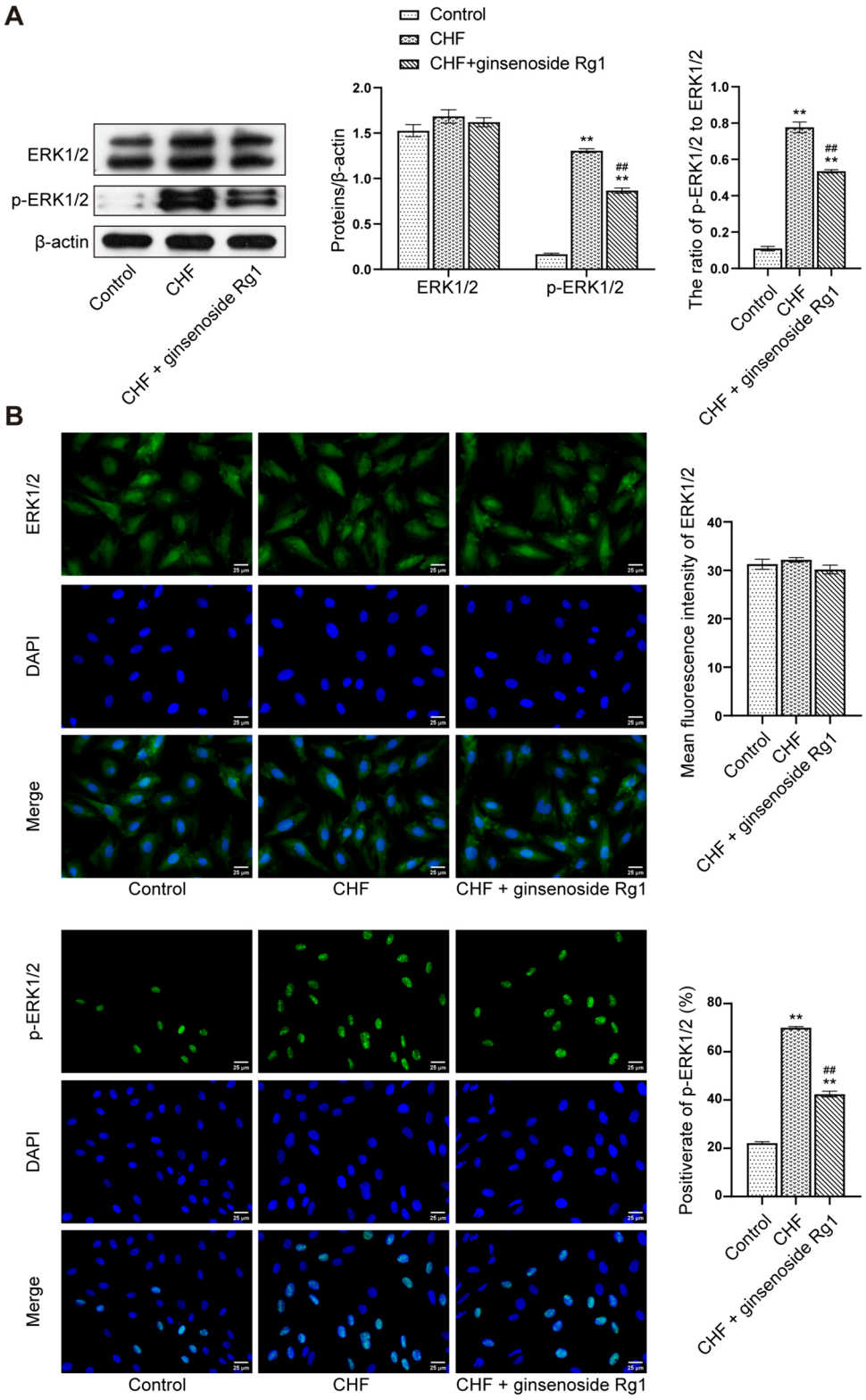

Figure 3. Modulation of ERK1/2 protein phosphorylation by GRg1. (*A*) Analysis of ERK1/2 and p-ERK1/2 protein expression levels in cardiomyocytes using Western blotting. (*B*) IF assay demonstrating positive signals of ERK1/2 and p-ERK1/2 displayed as *green fluorescence*, with nuclear staining signals represented in *blue coloration*. Positive rate of p-ERK1/2 (%) and the mean fluorescence intensity of ERK1/2 were measured. (**$p < 0.01$ indicates significant comparisons to the normal control group, and $^{\#\#}p < 0.01$ indicates significant comparisons to the CHF (ADR) group).

mechanism, the expression levels of ERK1/2 and p-ERK1/2 were assessed using Western blotting. Additionally, IF staining was employed to examine the localization of p-ERK1/2 in myocardial tissue specimens from all rat groups, providing insights into the role of ERK1/2 protein phosphorylation in the treatment of CHF in rats using GRg1. Interestingly, Western blotting outcomes showed no notable variances in the expression levels of ERK1/2 in myocardial tissues across

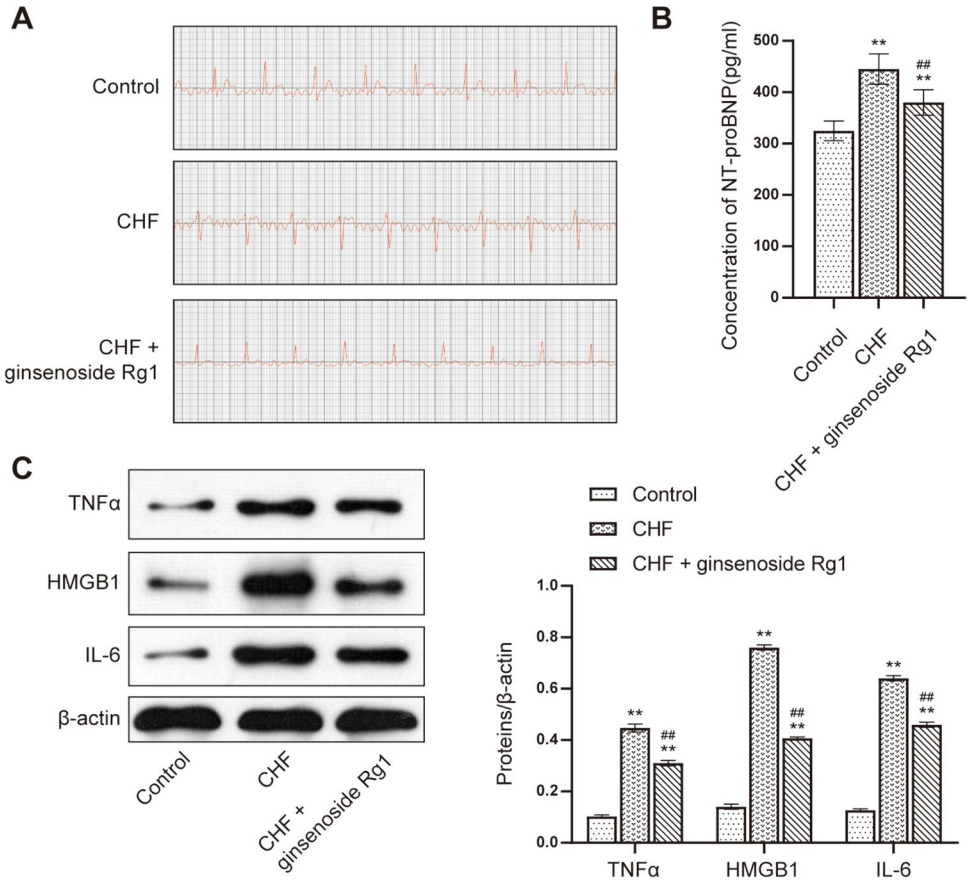

Figure 4. Cardioprotective effect of GRg1 in rats with CHF. (*A*) Electrocardiogram assessment. (*B*) Measurement of NT-proBNP levels in rat serum using ELISA. (*C*) Analysis of TNFα, HMGB1, and IL-6 expression levels as inflammatory factors in the heart through Western blotting. (**$p < 0.01$ denotes a substantial difference compared to the control group, ##$p < 0.01$ signifies a notable distinction in comparison to the CHF (ADR) group).

the different experimental groups. However, the expression of p-ERK1/2 was enhanced in both the CHF (ADR) group and the CHF+ginsenoside Rg1 group in comparison to the normal control group. Among these, p-ERK1/2 expression in the CHF (ARD) group was the highest ($p < 0.01$, Fig. 6*A*). IF staining corroborated these findings, demonstrating increased p-ERK1/2 expressions primarily within the nuclei of cells in the CHF (ADR) group (characterized by apparent translocation to the nucleus). The phosphorylation level of ERK1/2 protein was markedly increased in both the CHF (ADR) group and the CHF+ginsenoside Rg1 group, as compared to the control group. Besides, phosphorylation level of ERK1/2 protein was inhibited in the CHF+ ginsenoside Rg1 group compared with the CHF (ADR) group ($p < 0.01$, Fig. 6*B*).

Discussion

CHF is a multifaceted clinical syndrome that occurs in the advanced stages of various cardiovascular diseases (Heidenreich *et al*. 2022). It is characterized by a high prevalence, substantial mortality rate, and significant economic burden, making it a grave threat to human health. The underlying pathogenesis of CHF is intricate, and ventricular remodeling serves as a crucial physiological basis for its persistence. Throughout the progression of ventricular remodeling in CHF, there is excessive apoptosis of cardiomyocytes, leading to a decrease in cardiac contractile units. In this investigation, we have confirmed that GRg1 has the potential to inhibit the phosphorylation of ERK1/2 protein via the regulation of H9c2 cardiomyocyte proliferation. Simultaneously, GRg1 exhibited a dual effect by suppressing apoptosis and reducing the expression levels of inflammatory factors, namely TNFα, HMGB1, and IL-6. Consequently, these effects contributed to the mitigation of ventricular remodeling in CHF. Collectively, these discoveries emphasized the promise of GRg1 as a potential contender for future preventive and clinical interventions in the treatment of CHF.

GRg1 exhibits a wide range of effects, including antihypertensive properties, anti-myocardial fibrosis, prevention of cardiovascular remodeling, and attenuation of hypoxia/reoxygenation (H/R) injury (Fan *et al*. 2020; Zhu *et al*. 2021). These findings offer novel perspectives for the prevention and treatment of CHF in clinical settings. One of the primary benefits of GRg1 is its antioxidant activity, which safeguards the structural integrity of mitochondria and enhances the activity of adenosine triphosphate ATPase, ensuring a continuous energy supply to ischemic myocardial tissues.

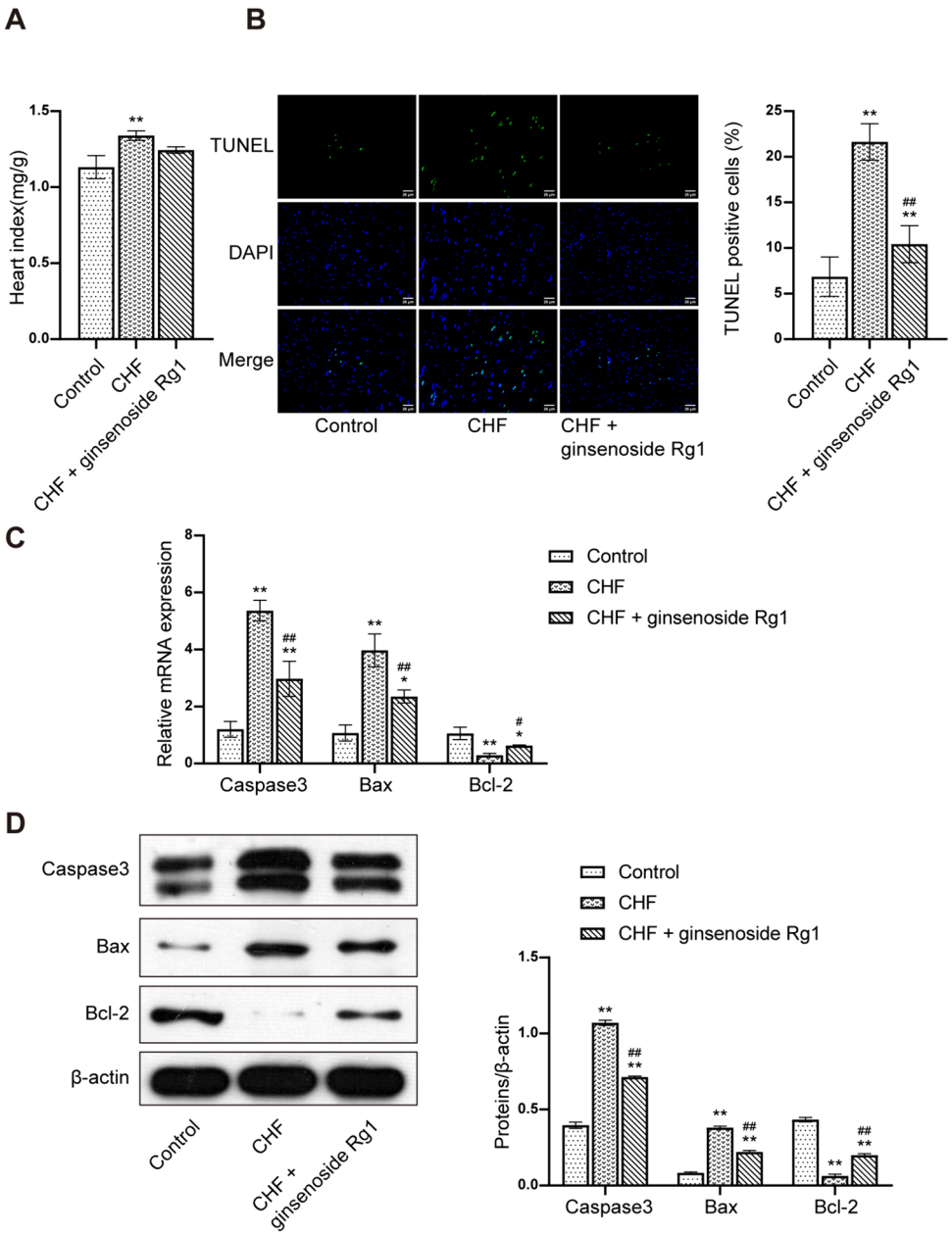

Figure 5. Impact of GRg1 on cardiac apoptosis in rats with CHF. (*A*) Assessment of HW/BW index in rats. (*B*) Evaluation of cardiomyocyte apoptosis rate using the TUNEL method. (*C*) Analysis of Caspase3, Bax, and Bcl-2 mRNA expression levels by RT-PCR. (*D*) Detection of Caspase3, Bax, and Bcl-2 protein expression levels by Western blotting. (**$p < 0.01$ and *$p < 0.05$ indicate significant comparisons to the control group, while $^{\#\#}p < 0.01$ and $^{\#}p < 0.05$ indicate significant comparisons to the CHF (ADR) group).

Additionally, GRg1 mitigates the production of mitochondrial reactive oxygen species (ROS) and protects cardiomyocytes against oxidative stress damage by scavenging free radicals (Yang *et al*. 2022). Studies have demonstrated that GRg1 reduces mitochondrial membrane depolarization and decreases ROS formation in isolated cardiomyocytes by downregulating the calpain-1 signaling pathway (Lu *et al*. 2021; Zhao *et al*. 2023). Furthermore, GRg1 has been observed to inhibit ventricular remodeling and slow down the progress of CHF by upregulating the expression of essential proteins involved in the SIRT1/PINK1/Parkin-mediated mitochondrial autophagy pathway (Guan *et al*. 2020; Guan *et al*. 2023).

Aside from its effects on the heart, GRg1 also demonstrates protective effects on vascular endothelial cells, offering resistance against atherosclerosis (Zhou *et al*. 2022). Researches have shown that GRg1 reduces cardiac injury by ameliorating thromboembolic pulmonary hypertension-induced myocardial remodeling, thereby diminishing cardiac damage (Li *et al*. 2013; Li *et al*. 2017). Moreover, GRg1 has the capacity to alleviate sepsis-induced myocardial dysfunction by reducing the inward flow of Ca^{2+} and increasing mitochondrial membrane potential through the Akt/GSK-3β signaling axis triggered by the p2x7 receptor (Liu *et al*. 2022b). In a study conducted by Li C *et al*., Dox@rg1 nanoparticles were engineered utilizing self-assembled

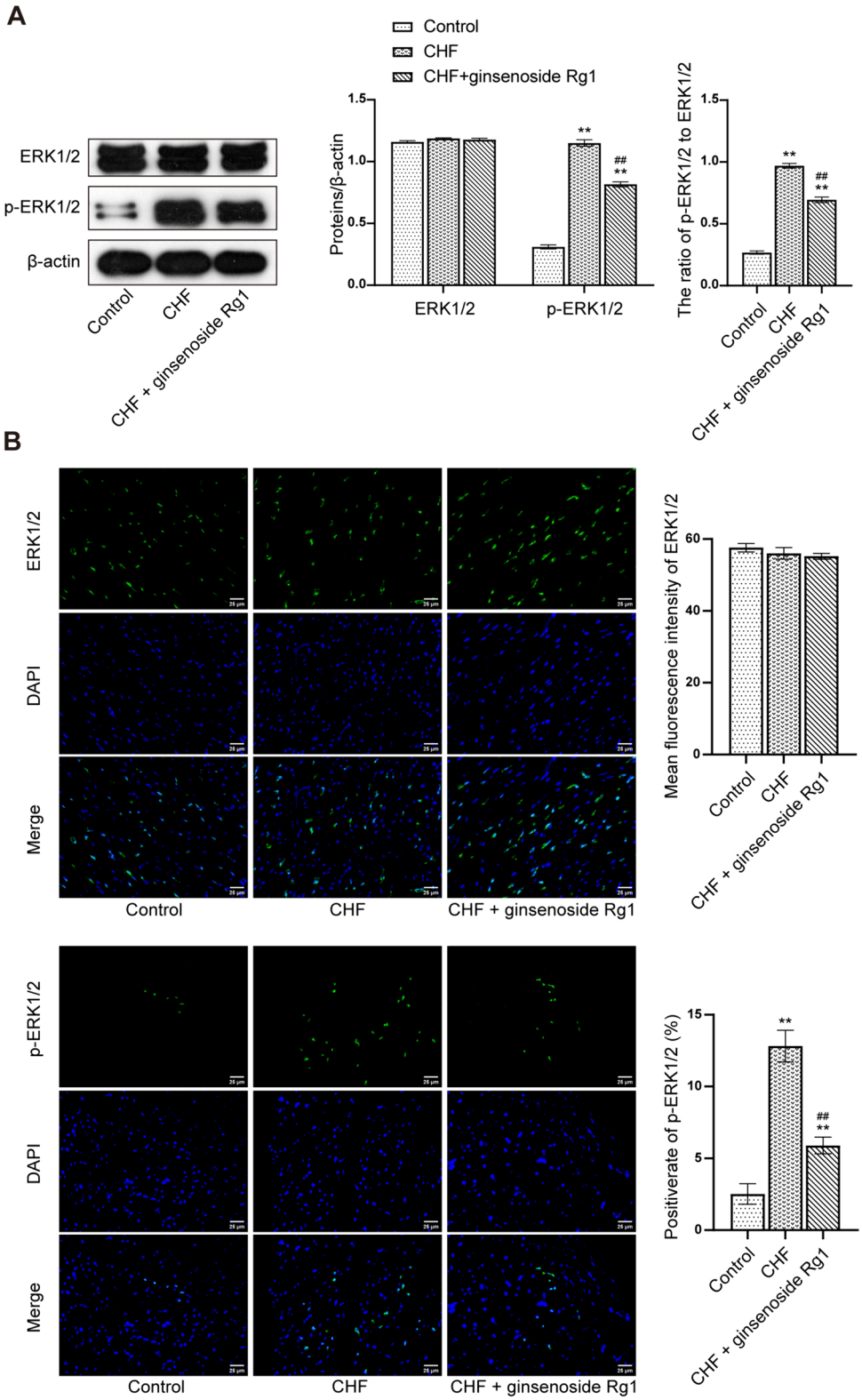

Figure 6. The regulatory effect of GRg1 on ERK1/2 protein phosphorylation in rat hearts with CHF. (*A*) Investigation of ERK1/2 and p-ERK1/2 protein expression levels using Western blotting. (*B*) IF staining to assess the expression of ERK1/2 and p-ERK1/2. Positive rate of p-ERK1/2 (%) and the mean fluorescence intensity of ERK1/2 were measured. (**$p < 0.01$ denotes a notable distinction in comparison to the control group, $^{\#\#}p < 0.01$ indicates a significant difference when compared to the CHF (ADR) group).

GRg1 as a carrier, and ADR was encapsulated on its surface (Li *et al*. 2021). The results confirmed the effective mitigation of ADR-induced cardiotoxicity in 4T1 hormonal mice by GRg1. Luo M *et al*. demonstrated that GRg1 inhibited cardiac inflammation and apoptosis by obstructing the TLR4/NF-κB/NLRP3 pathway (Luo *et al*. 2020). Furthermore, experimental evidence supports the proposition that GRg1 protects cardiomyocytes from hypoxic injury by

activating the PI3K/AKT/mTOR pathway and elevating the levels of HIF-1α expression (Qin *et al*. 2018).

ERK1/2, as the extensively studied components of the MAPK pathway, play vital roles in regulating cell apoptosis and survival. They are particularly implicated in cell proliferation and exert their influence on the cell growth cycle through three distinct pathways: stimulating DNA synthesis, promoting cell cycle progression, and enhancing the activity of transcription factors (LIU Rui 2012). Typically, ERK1/2 modulate upstream factors involved in apoptotic events by interacting with downstream transcription factors, which consequently triggers the release of cytochrome C. ERK1/2 decreases the levels of the anti-apoptotic protein Bcl-2 while increasing the expression of the pro-apoptotic protein Bax. This activation ultimately leads to upregulation of apoptotic genes such as Caspase3, 8, and 9 (Sun *et al*. 2015). Under stressful conditions, the activation of the ERK1/2 signaling pathway plays a pivotal protective role in CHF myocardium by inhibiting cell apoptosis and preventing necrosis. Remarkably, a study has demonstrated that targeted activation of ERK1/2 protein phosphorylation can reduce mitochondrial fission and enhance membrane potential, thus alleviating myocardial ischemia-reperfusion (I/R) injury caused by high blood glucose levels (Yu *et al*. 2022). In vitro research conducted by Wu W *et al*. suggests that dexmedetomidine may enhance telomere/telomerase function via the ERK1/2-Nrf2 pathway, thereby mitigating hypoxia-induced cardiomyocyte injury (Wu *et al*. 2022). In the study conducted by Zhao Q *et al*., AAV9-CaMEK was found to hinder mitochondrial fragmentation to some extent by activating the ERK1/2 signaling pathway, thereby counteracting ischemia-induced heart failure in aged subjects (Zhao *et al*. 2021). Interestingly, a related report has observed that the inhibitory effects of ERK1/2 inhibitors on myocardial I/R injury were amplified when combined with Baicalein, leading to reduced cardiomyocyte survival (Liu *et al*. 2020). Numerous investigations have highlighted the significant correlation between attenuated activation of ERK1/2 and eccentric hypertrophy induced by volume overload (Jochmann *et al*. 2019). Sun MH *et al*. conducted a study showcasing the myocardial protection provided by CaMEK, which inhibits apoptosis and mitochondrial autophagy induced by H_20_2 through the activation of ERK1/2 phosphorylation (Sun *et al*. 2019).

In the present study, the findings emphasized the impact of GRg1 on the survival and proliferative activity of cardiomyocyte in the context of ADR-induced condition. The results obtained from MTT assay and EdU analysis revealed a noteworthy reduction in cardiomyocyte survival under the ADR-induced state. However, when GRg1 was administered, a notable increase in the proliferative activity of cardiomyocytes was observed, along with a reduction in myocardial injury. Furthermore, the outcomes derived from flow cytometry, RT-qPCR, and Western blotting assays provided evidence that GRg1 effectively suppressed cardiomyocyte apoptosis and alleviated myocardial inflammation in rats with CHF. IF staining results provided additional insights, suggesting that GRg1 may regulate CHF by inhibiting ERK1/2 protein phosphorylation. The cardioprotective effect of GRg1 on CHF was further confirmed through electrocardiography and ELISA detection of NT-proBNP content in rat serum. Remarkably, the HW/BW index and TUNEL assay served as complementary evidence, supporting the inhibitory role of GRg1 in ventricular remodeling and its impact on the progression of CHF in rats.

Conclusion

In summary, this study provided compelling evidence to support the therapeutic potential of GRg1 in the treatment of CHF. First and foremost, GRg1 exhibited the ability to promote cell proliferation by inhibiting the phosphorylation of ERK1/2 proteins. Moreover, the study showcased the protective properties of GRg1 against cardiomyocyte apoptosis and cardiac inflammation. These findings underscored the promising prospects of GRg1 as a promising treatment for CHF.

Funding This study was supported by the Scientific Research Project of Traditional Chinese Medicine in Hunan Province (B2023026), the Scientific Research Program of Hunan Provincial Health Commission (202203015711), the Open Fund Project of Integrative Medicine of Hunan Province "Domestic First-class Cultivation Disciplines" (2020ZXYJH74), the National Innovation and Entrepreneurship Training Program for College Students (202210541012), and the Innovation and Entrepreneurship Training Program for College Students in Hunan Province (2022-2857).

Data Availability The data used and analyzed in this study are available from the corresponding author upon reasonable request.

Declarations

Ethics approval The experimental procedures strictly adhered to the regulations set by the Animal Protection Committee of Hunan University of Chinese Medicine. The Ethics Committee of Hunan University of Chinese Medicine granted approval for the experimental protocol (Ethics Approval No. LL2022091001).

Conflict of interest The authors declare no competing interests.

References

Cai J, Huang K, Han S, Chen R, Li Z, Chen Y, Chen B, Li S, Xinhua L, Yao H (2022) A comprehensive system review of pharmacological effects and relative mechanisms of Ginsenoside Re: recent advances and future perspectives. Phytomed 102:154119

Fan W, Huang Y, Zheng H, Li S, Li Z, Yuan L, Cheng X, He C, Sun J (2020) Ginsenosides for the treatment of metabolic syndrome and cardiovascular diseases: pharmacology and mechanisms. Biomed Pharmacother 132:110915

Guan S, Xin Y, Ding Y, Zhang Q, Han W (2023) Ginsenoside Rg1 protects against cardiac remodeling in heart failure via SIRT1/PINK1/Parkin-mediated mitophagy. Chem Biodivers 20:e202200730

Guan S, Yu P, Cao J, Xi X, Zhang Q, Zhu C, Hu H, Gong X, Fan H (2020) Ginsenoside Rg1 protects against cigarette smoke-induced airway remodeling by suppressing the TGF-β1/Smad3 signaling pathway. Am J Transl Res 12:493–506

He J, Li YL (2015) Ginsenoside Rg1 downregulates the shear stress induced MCP-1 expression by inhibiting MAPK signaling pathway. Am J Chin Med 43:305–17

He SF, Jin SY, Yang W, Pan YL, Huang J, Zhang SJ, Zhang L, Zhang Y (2018) Cardiac μ-opioid receptor contributes to opioid-induced cardioprotection in chronic heart failure. Br J Anaesth 121:26–37

Heidenreich PA, Bozkurt B, Aguilar D, Allen LA, Byun JJ, Colvin MM, Deswal A, Drazner MH, Dunlay SM, Evers LR, Fang JC, Fedson SE, Fonarow GC, Hayek SS, Hernandez AF, Khazanie P, Kittleson MM, Lee CS, Link MS, Milano CA, Nnacheta LC, Sandhu AT, Stevenson LW, Vardeny O, Vest AR, Yancy CW (2022) 2022 AHA/ACC/HFSA guideline for the management of heart failure: a report of the American College of Cardiology/American Heart Association Joint Committee on Clinical Practice Guidelines. Circulation 145:e895–e1032

Huang CY, Lee FL, Peng SF, Lin KH, Chen RJ, Ho TJ, Tsai FJ, Padma VV, Kuo WW, Huang CY (2018) HSF1 phosphorylation by ERK/GSK3 suppresses RNF126 to sustain IGF-IIR expression for hypertension-induced cardiomyocyte hypertrophy. J Cell Physiol 233:979–989

Huang L, Liu LF, Liu J, Dou L, Wang GY, Liu XQ, Yuan QL (2016) Ginsenoside Rg1 protects against neurodegeneration by inducing neurite outgrowth in cultured hippocampal neurons. Neural Regen Res 11:319–25

Jochmann S, Elkenani M, Mohamed BA, Buchholz E, Lbik D, Binder L, Lorenz K, Shah AM, Hasenfuß G, Toischer K, Schnelle M (2019) Assessing the role of extracellular signal-regulated kinases 1 and 2 in volume overload-induced cardiac remodelling. ESC Heart Fail 6:1015–1026

Ju S, Park S, Lim L, Choi DH, Song H (2020) Low density lipoprotein receptor-related protein 1 regulates cardiac hypertrophy induced by pressure overload. Int J Cardiol 299:235–242

Li C, Gou X, Gao H (2021) Doxorubicin nanomedicine based on ginsenoside Rg1 with alleviated cardiotoxicity and enhanced antitumor activity. Nanomed (Lond) 16:2587–2604

Li CY, Deng W, Liao XQ, Deng J, Zhang YK, Wang DX (2013) The effects and mechanism of ginsenoside Rg1 on myocardial remodeling in an animal model of chronic thromboembolic pulmonary hypertension. Eur J Med Res 18:16

Li Q, Xiang Y, Chen Y, Tang Y, Zhang Y (2017) Ginsenoside Rg1 protects cardiomyocytes against hypoxia/reoxygenation injury via activation of Nrf2/HO-1 signaling and inhibition of JNK. Cell Physiol Biochem 44:21–37

Liu Rui GW (2012) Mitogen-activated protein kinase signalling pathway and its role in apoptosis. Chin J Gerontol 32:4089–4092

Liu S, Huang J, Gao F, Yin Z, Zhang R (2022a) Ginsenoside RG1 augments doxorubicin-induced apoptotic cell death in MDA-MB-231 breast cancer cell lines. J Biochem Mol Toxicol 36:e22945

Liu X, Zhang S, Xu C, Sun Y, Sui S, Zhang Z, Luan Y (2020) The protective of baicalin on myocardial ischemia-reperfusion injury. Curr Pharm Biotechnol 21:1386–1393

Liu Z, Pan H, Zhang Y, Zheng Z, Xiao W, Hong X, Chen F, Peng X, Pei Y, Rong J, He J, Zou L, Wang J, Zhong J, Han X, Cao Y (2022b) Ginsenoside-Rg1 attenuates sepsis-induced cardiac dysfunction by modulating mitochondrial damage via the P2X7 receptor-mediated Akt/GSK-3β signaling pathway. J Biochem Mol Toxicol 36:e22885

Lu ML, Wang J, Sun Y, Li C, Sun TR, Hou XW, Wang HX (2021) Ginsenoside Rg1 attenuates mechanical stress-induced cardiac injury via calcium sensing receptor-related pathway. J Ginseng Res 45:683–694

Lu XL, Tong YF, Liu Y, Xu YL, Yang H, Zhang GY, Li XH, Zhang HG (2015) Gαq protein carboxyl terminus imitation polypeptide GCIP-27 improves cardiac function in chronic heart failure rats. PLoS One 10:e0121007

Luo M, Yan D, Sun Q, Tao J, Xu L, Sun H, Zhao H (2020) Ginsenoside Rg1 attenuates cardiomyocyte apoptosis and inflammation via the TLR4/NF-kB/NLRP3 pathway. J Cell Biochem 121:2994–3004

McDonagh TA, Metra M, Adamo M, Gardner RS, Baumbach A, Böhm M, Burri H, Butler J, Čelutkienė J, Chioncel O, Cleland JGF, Coats AJS, Crespo-Leiro MG, Farmakis D, Gilard M, Heymans S, Hoes AW, Jaarsma T, Jankowska EA, Lainscak M, Lam CSP, Lyon AR, Mcmurray JJV, Mebazaa A, Mindham R, Muneretto C, Francesco Piepoli M, Price S, Rosano GMC, Ruschitzka F, Kathrine Skibelund A (2021) 2021 ESC guidelines for the diagnosis and treatment of acute and chronic heart failure. Eur Heart J 42:3599–3726

Qin L, Fan S, Jia R, Liu Y (2018) Ginsenoside Rg1 protects cardiomyocytes from hypoxia-induced injury through the PI3K/AKT/mTOR pathway. Pharmazie 73:349–355

Stretti L, Zippo D, Coats AJS, Anker MS, Von Haehling S, Metra M, Tomasoni D (2021) A year in heart failure: an update of recent findings. ESC Heart Fail 8:4370–4393

Sun MH, Chen XC, Han M, Yang YN, Gao XM, Ma X, Huang Y, Li XM, Gai MT, Liu F, Ma YT, Chen BD (2019) Cardioprotective effects of constitutively active MEK1 against H(2)O(2)-induced apoptosis and autophagy in cardiomyocytes via the ERK1/2 signaling pathway. Biochem Biophys Res Commun 512:125–130

Sun Y, Liu WZ, Liu T, Feng X, Yang N, Zhou HF (2015) Signaling pathway of MAPK/ERK in cell proliferation, differentiation, migration, senescence and apoptosis. J Recept Signal Transduct Res 35:600–4

Sun Y, Yang Y, Liu S, Yang S, Chen C, Lin M, Zeng Q, Long J, Yao J, Yi F, Meng L, Ai Q, Chen N (2022) New therapeutic approaches to and mechanisms of ginsenoside Rg1 against neurological diseases. Cell 11. https://doi.org/10.3390/cells11162529

Wang Y, Guo Z, Gao Y, Liang P, Shan Y, He J (2019) Angiotensin II receptor blocker LCZ696 attenuates cardiac remodeling through the inhibition of the ERK signaling pathway in mice with pregnancy-associated cardiomyopathy. Cell Biosci 9:86

Wu W, Du Z, Wu L (2022) Dexmedetomidine attenuates hypoxia-induced cardiomyocyte injury by promoting telomere/telomerase activity: possible involvement of ERK1/2-Nrf2 signaling pathway. Cell Biol Int 46:1036–1046

Xie W, Zhou P, Sun Y, Meng X, Dai Z, Sun G, Sun X (2018) Protective effects and target network analysis of ginsenoside Rg1 in cerebral ischemia and reperfusion injury: a comprehensive overview of experimental studies. Cells 7. https://doi.org/10.3390/cells7120270

Xu ZM, Li CB, Liu QL, Li P, Yang H (2018) Ginsenoside Rg1 prevents doxorubicin-induced cardiotoxicity through the inhibition of autophagy and endoplasmic reticulum stress in mice. Int J Mol Sci 19. https://doi.org/10.3390/ijms19113658

Yan ZP, Li JT, Zeng N, Ni GX (2021) Role of extracellular signal-regulated kinase 1/2 signaling underlying cardiac hypertrophy. Cardiol J 28:473–482

Yang C, Jiang G, Xing Y (2022) Protective effect of ginsenosides Rg1 on ischemic injury of cardiomyocytes after acute myocardial infarction. Cardiovasc Toxicol 22:910–915

Yang HL, Hsieh PL, Hung CH, Cheng HC, Chou WC, Chu PM, Chang YC, Tsai KL (2020) Early moderate intensity aerobic exercise intervention prevents doxorubicin-caused cardiac dysfunction through inhibition of cardiac fibrosis and inflammation. Cancers (Basel) 12. https://doi.org/10.3390/cancers12051102

Ye J, Yan S, Liu R, Weng L, Jia B, Jia S, Xiong Y, Zhou Y, Leng M, Zhao J, Yang F, Zheng M (2023) CMTM3 deficiency induces cardiac hypertrophy by regulating MAPK/ERK signaling. Biochem Biophys Res Commun 667:162–169

Yu F, Liu F, Luo JY, Zhao Q, Wang HL, Fang BB, Li XM, Yang YN (2022) Targeted activation of ERK1/2 reduces ischemia and reperfusion injury in hyperglycemic myocardium by improving mitochondrial function. Ann Transl Med 10:1238

Yu H, Zhen J, Yang Y, Gu J, Wu S, Liu Q (2016) Ginsenoside Rg1 ameliorates diabetic cardiomyopathy by inhibiting endoplasmic reticulum stress-induced apoptosis in a streptozotocin-induced diabetes rat model. J Cell Mol Med 20:623–31

Yuan C, Wang H, Yuan Z (2019) Ginsenoside Rg1 inhibits myocardial ischaemia and reperfusion injury via HIF-1 α-ERK signalling pathways in a diabetic rat model. Pharmazie 74:157–162

Zhang S, Zhao Y, Tan L, Wu S, Zhang Q, Zhao B, Li G (2022) A Novel Berberine-glycyrrhizic acid complex formulation enhanced the prevention effect to doxorubicin-induced cardiotoxicity by pharmacokinetic modulation of berberine in rats. Front Pharmacol 13:891829

Zhao F, Lu M, Wang H (2023) Ginsenoside Rg1 ameliorates chronic intermittent hypoxia-induced vascular endothelial dysfunction by suppressing the formation of mitochondrial reactive oxygen species through the calpain-1 pathway. J Ginseng Res 47:144–154

Zhao Q, Liu F, Zhao Q, Zhang J, Luo J, Li X, Yang Y (2021) Constitutive activation of ERK1/2 signaling protects against myocardial ischemia via inhibition of mitochondrial fragmentation in the aging heart. Ann Transl Med 9:479

Zhou Q, He X, Zhao X, Fan Q, Lai S, Liu D, He H, He M (2022) Ginsenoside Rg1 ameliorates acute renal ischemia/reperfusion injury via upregulating AMPKα1 expression. Oxid Med Cell Longev 2022:3737137

Zhouming X, L. J., Xueqi L, Haixia T, Tao B, Rong H (2021) Research progress on myocardial hypertrophy signal transduction pathways. *Medical Recapitulate,* 27**,** 29-35

Zhu C, Wang Y, Liu H, Mu H, Lu Y, Zhang J, Huang J (2017) Oral administration of ginsenoside Rg1 prevents cardiac toxicity induced by doxorubicin in mice through anti-apoptosis. Oncotarget 8:83792–83801

Zhu GX, Zuo JL, Xu L, Li SQ (2021) Ginsenosides in vascular remodeling: cellular and molecular mechanisms of their therapeutic action. Pharmacol Res 169:105647